

## Supplementary Information for:

# Improved Ligand-assisted Reprecipitation Method Synthesized Aqueous-phase CsPbBr<sub>3</sub> Perovskite Nanocrystals and Their Electrochemiluminescence Behavior

Xiaodong Luan,<sup>ad‡</sup> Shuochen Fan,<sup>a‡</sup> Ke Xu,<sup>b</sup> Haipeng Zhang,<sup>a</sup> Xiaoyang Feng,<sup>b</sup> Wenteng Zhang,<sup>b</sup> Huaping Peng <sup>\*c</sup> and Qile Li <sup>\*b</sup>

<sup>a</sup> School of Electrical and Electronic Engineering, Jiangsu Ocean University, Lianyungang 222005, China.

<sup>b</sup> School of Science, Jiangsu Ocean University, Lianyungang 222005, China. E-mail: [2017000021@jou.edu.cn](mailto:2017000021@jou.edu.cn)

<sup>c</sup> Fujian Key Laboratory of Drug Target Discovery and Structural and Functional Research, School of Pharmacy, Fujian Medical University, Fuzhou 350004, China. E-mail: [penghuaping@fjmu.edu.cn](mailto:penghuaping@fjmu.edu.cn)

<sup>d</sup> Jiangsu Institute of Marine Resources Development, Lianyungang 222005, China.

<sup>‡</sup> Both authors contributed equally to this work.

### Chemicals and Reagents

The raw materials for the synthesis of CsPbBr<sub>3</sub> NCs used in this paper are cesium trifluoroacetate (Cs-TFA, 98%; Alfa Aesar), lead bromide (PbBr<sub>2</sub>, 99.999%), cesium bromide (CsBr, 99.99%), N-N-dimethylacetamide (DMA, 99.9%), 4-bromo-butyric acid (BBA, 98%), and oleylamine (OLA, 80-90%). They were purchased from Aladdin Chemical Reagent Co., Ltd.

The materials for electrochemiluminescence (ECL) detection of TFA-BBA-CPB NCs employed in this paper are N-N-Diethyl-ethanamine (TEA), potassium peroxydisulfate (K<sub>2</sub>S<sub>2</sub>O<sub>8</sub>), Na<sub>2</sub>HPO<sub>4</sub>, and NaH<sub>2</sub>PO<sub>4</sub>. They were purchased from Sinopharm Chemical Reagent Co. Ltd. (Shanghai, China). Tetrachloroauric (III) acid tetrahydrate (HAuCl<sub>4</sub>·4H<sub>2</sub>O), N-acetyl-L-cysteine (NAC), sodium borohydride (NaBH<sub>4</sub>), L-glutathione reduced (GSH), Histidine (His), and acetyl choline (AChE) were purchased from Aladdin Reagent Company (Shanghai, China). Ascorbic acid (AA), glucose (Glu), and urea were obtained from Sinopharm Chemical Reagent Co. Ltd. (Shanghai, China). Potassium permanganate (KMnO<sub>4</sub>) was obtained from Lisheng Chemical Reagent Co. Ltd. (Shanghai, China). 0.1 M phosphate buffer solutions (PBS, pH 7.4) containing 0.1 M K<sub>2</sub>S<sub>2</sub>O<sub>8</sub> as coreactant was used as electrolyte in electrochemistry and ECL analysis. Ultrapure water was fabricated in the laboratory by AFX-1002-U. All chemical reagents were of analytical grade and used directly without further purification.

### W-LARP method Synthesized aqueous-phase CsPbBr<sub>3</sub> NCs

The entire synthesis procedure was carried out via a ligand-assisted reprecipitation method in water without using any inert gas (Fig. S1). 0.8 mmol Cs-TFA and 0.4 mmol PbBr<sub>2</sub> were added to a transparent reagent bottle containing 10 mL DMA solutions. The mixed solutions were warmed to 60 °C and kept under magnetic stirring for 50 min. Subsequently, 2 mmol OLA and 2 mmol BBA solutions were successively and rapidly injected into the above solutions. In order to make the ligands react entirely, it is crucial to continue heating and stirring for 15 min. Then, 1 mL of the precursor was quickly injected into 12 mL aqueous solutions within 10 seconds under vigorous stirring at 60 °C. The reaction mixture was centrifuged at 5000 rpm for 10 min, and the yellow precipitate solid at the bottom of the centrifugal tube was discarded. The supernatant was kept clear after being centrifuged at 10000 rpm for 15 min again. After centrifugation, the supernatant was retained for subsequent characterization.

In addition, we also synthesized CsPbBr<sub>3</sub> NCs employing PbBr<sub>2</sub> and CsBr to compare our work in aqueous solutions, and the whole synthesis step was similar to the synthesis of TFA-BBA-CsPbBr<sub>3</sub> NCs. 0.4 mmol CsBr and 0.4 mmol PbBr<sub>2</sub> were added to a transparent reagent bottle containing 10 mL DMA solutions, heated to 60 °C, and kept under magnetic stirring for 50 min. Subsequently, 2 mmol OLA and 2 mmol BBA solutions were continuously and rapidly injected into the above solutions. In order to make the ligands react entirely, it is vital to continue heating and stirring for 15 min. Then, 1 mL of the precursor was quickly injected into 12 mL aqueous solutions within 10 seconds under vigorous stirring at 60 °C. The reaction mixture was centrifuged at 5000 rpm for 10 min, and the yellow precipitate solid in the bottom of the centrifugal tube was discarded. The supernatant was removed and centrifuged at 10000 rpm for 15 min. After centrifugation, the supernatant was retained for subsequent characterization.<sup>1,2</sup>

### First-principles calculation setting

First-principles calculations based on density functional theory (DFT) were carried out via the Vienna ab-initio simulation package (VASP), and the crystal model of CsPbBr<sub>3</sub> NCs was constructed using Materials Studio.<sup>3,4</sup> The projected augmented wave was employed to resolve the ion-electron exchange interaction potential in the system, and the electron exchange-correlation function adopted the generalized gradient approximation. Meanwhile, the exchange-correlation energy applied to the Perdew-Burke-Ernzerhof (PBE) functional, and the ultrasoft pseudopotential calculated the relevant pseudopotential. Subsequently, the plane wave truncation

energy was set to 450.0 eV, and the static self-consistency convergence threshold was selected to  $5.0 \times 10^{-7}$  eV/atom in the calculation process. The electronic structure converged, and the static self-consistent field was terminated when the energy difference between adjacent electron steps was less than or equal to  $10^{-5}$  eV/atom. The atomic positions need to be fully optimized in the crystal structure. Meanwhile, the electronic and crystal structure optimization was completed when all atomic residual stress components were less than  $0.01$  eV/Å. In this case, the Brillouin zone integration was performed a  $3 \times 3 \times 1$  Monkhorst-Pack grid with a Gaussian spread set to  $0.05$  eV. The adsorption energy was calculated by using the following equation.

$$E_{\text{ads}} = E_{\text{total}} - E_{\text{sub}} - E_{\text{mol}} \quad \backslash * \text{MERGEFORMAT (1)}$$

Where  $E_{\text{ads}}$  indicates the adsorption energy of the substrate on the adsorbate.  $E_{\text{total}}$  is the total energy of the substrate and the adsorbate. Meanwhile,  $E_{\text{sub}}$  is the energy of the substrate, together with  $E_{\text{mol}}$  is the energy of the adsorbed molecular.<sup>5</sup>

#### Preparation of TFA-BBA-CPB NCs|GCE

Glassy carbon electrodes (GCE, 3 mm diameter, CH Instruments, Inc.) were wet-polished primarily with  $0.3$  and  $0.05$   $\mu\text{m}$  alumina slurry and then cleaned thoroughly with ultrapure water. Subsequently, the GCEs were sequentially sonicated in 1:1 nitric acid, ethanol, and double-distilled water and then dried in air at room temperature. Afterward,  $2.5$   $\mu\text{L}$  of TFA-BBA-CPB NCs solution was dropped on the surface of the GCE and dried at room temperature. The modified electrode was designated as TFA-BBA-CPB NCs|GCE.<sup>6</sup>

#### Preparation of MnO<sub>2</sub>|TFA-BBA-CPB NCs|GCE

MnO<sub>2</sub> was electrodeposited on the surface of TFA-BBA-CPB NCs|GCE via chronoamperometry method at  $-0.2$  V for  $300$  s in the mixture solution of  $20$  mM KMnO<sub>4</sub> and  $90$  mM H<sub>2</sub>SO<sub>4</sub> (V/V=1:1). The resulting electrode was recorded as MnO<sub>2</sub>|TFA-BBA-CPB NCs|GCE and rinsed thoroughly with distilled water. Subsequently, the electrode was dried with N<sub>2</sub> immediately for characterization and application.

#### The detection process of GSH

$100$   $\mu\text{L}$  of  $1$   $\mu\text{M}$  GSH solution was taken in an Eppendorf tube, and MnO<sub>2</sub>|TFA-BBA-CPB NCs|GCE was placed and incubated for  $10$  min. Subsequently, the electrode was gently rinsed with PBS (pH 7.4) and dried naturally.<sup>7</sup>

#### The test procedure of ECL

The ECL signals were obtained through ECL transient technology with stepping the potential from  $0$  V to  $-2$  V in  $0.1$  M PBS (pH 7.4) containing  $0.1$  M K<sub>2</sub>S<sub>2</sub>O<sub>8</sub>. The pulse periods at  $-2$  V and  $0$  V were  $1$  s and  $10$  s, respectively. The change in ECL intensity ( $\Delta I$ ) was calculated using the following equation.

$$\Delta I = (I_2 - I_1) / I_0 \quad \backslash * \text{MERGEFORMAT (2)}$$

where  $I_0$  stands for the ECL intensity of TFA-BBA-CPB NCs|GCE.  $I_1$  represents the ECL intensity of MnO<sub>2</sub>|TFA-BBA-CPB NCs|GCE, and  $I_2$  stands for the ECL intensity of MnO<sub>2</sub>|TFA-BBA-CPB NCs|GCE treated with the GSH.

#### Design of interference experiment

Five potential interfering substances in blood were selected to formulate solutions, e.g., AA, Glu, His, Urea, and AchE. Afterward, the reaction system was added with the above substances to detect the change in ECL values, examining the specificity and selectivity of the design for the detection of GSH. Where,  $C_{\text{interfering substance}} = 1.0 \times 10^{-5}$  M,  $C_{\text{GSH}} = 1.0 \times 10^{-6}$  M.

#### Instrument and Apparatus

The morphology of the samples was investigated by transmission electron microscope (TEM) and high-resolution transmission electron microscope (HRTEM) (F200X G2, FEI Talos, America). The X-ray diffraction (XRD) patterns for phase evolution were obtained through the nickel-filtered Cu K $\alpha$  radiation in the  $2\theta$  range  $10$ - $60^\circ$  at a scan speed of  $1.0^\circ$   $2\theta$   $\text{min}^{-1}$  (Ultima IV, Rigaku, Japan). Phase identification was made using standard files. Fourier transform infrared spectroscopy (FTIR) was carried out on an FTIR spectrometer (Nicolet iS-10, Thermo Fisher Scientific, America). The X-ray photoelectron spectroscopy (XPS) was utilized employing an X-ray electron spectrometer (ESCALAB Xi+, Thermo Scientific, America) equipped with an Al K $\alpha$  source. The Ultraviolet-Visible (UV-Vis) absorption spectra were measured by employing a UV-Vis spectrophotometer (UV-1800PC, Shanghai MEPULDA Instrument Co., China). A fluorescence spectrophotometer (WFY-28, Tianjin Topu Instrument Co., China) was adopted to record the photoluminescence (PL) spectra at room temperature using a  $0.5$  W  $405$  nm laser as the excitation source. Fluorescence lifetimes were carried out using a fluorescent lifetime spectrometer (FLS1000, Edinburgh, Britain) based on a time-correlated single photon counting technique under a picosecond pulsed diode laser excitation of  $375$  nm. Ultraviolet photoelectron spectroscopy (UPS) measurements of TFA-BBA-CsPbBr<sub>3</sub> NCs was measured in an ultrahigh-vacuum chamber with a 4D beamline equipped with an electron analyzer and heating element (Thermo ESCALAB 250XI). Results were corrected for charging effects using an Au internal reference. The ECL measurement was measured through an RFAS-1 automatic electrochemiluminescence spectrophotometer (Xi'an Remex Analysis Instrument Co. Ltd. Xi'an, China) with a three-electrode system where a modified GCE was used as the working electrode, a Pt wire as the counter electrode, and Ag/AgCl as the reference electrode. The photomultiplier

---

tube (PMT) was biased at 850 V in the experiments. Cyclic voltammetry (CV) was recorded with a CHI660C electrochemical analyzer (Shanghai, China). All experiments were carried out at room temperature.

## Table of Contents

**Table S1.** The respective energies of  $\text{CF}_3\text{CO}_2^-$ , BBA and  $\text{CsPbBr}_3$  and the adsorption energy.

**Fig. S1** Synthesis methods of TFA-BBA-CPB NCs in aqueous solutions.

**Fig. S2** Sample photographs of TFA-BBA-CPB NCs and BBA-CPB NCs under natural light and UV light irradiation at 365 nm excitation wavelength with time.

**Fig. S3** Mechanistic investigations of TFA-BBA-CPB NCs and BBA-CPB NCs in aqueous solutions.

**Fig. S4** XPS energy spectrum of F 1s in TFA-BBA-CPB NCs.

**Fig. S5** Crystal structure model of CPB NCs before and after the introduction of BBA.

**Fig. S6** Sample photographs of TFA-BBA-CPB NCs in quartz cuvette under natural light and UV irradiation at 365 nm excitation wavelength. The UV-vis absorption spectra and the fluorescence emission spectra of TFA-BBA-CPB NCs. The fluorescence emission spectra of BBA-CPB NCs in aqueous solutions.

**Fig. S7** TRPL decay spectrum at 518 nm under the excitation of 375 nm for TFA-BBA-CPB NCs.

**Fig. S8** UPS spectra of TFA-BBA-CPB NCs in the photoemission cutoff and Fermi edge. UV-vis absorption spectrum of TFA-BBA-CPB NCs. Schematic representation of the band structure for TFA-BBA-CPB NCs at the interface.

**Fig. S9** CVs of TFA-BBA-CPB NCs|GCE in air-free 0.1 M pH 7.4 PBS containing 0.1 M  $\text{K}_2\text{S}_2\text{O}_8$  and 0.2 M TEA at a scan rate of 0.1 V/s. ECL-time curve of TFA-BBA-CPB NCs with a potential window between 0.0 V and -2.0 V or +2.0 V.

**Fig. S10** ECL-time curves of TFA-BBA-CPB NCs before, during (the 14th circle), and after ECL measurements. The changes of ECL intensity of TFA-BBA-CPB NCs|GCE,  $\text{MnO}_2$ |TFA-BBA-CPB NCs|GCE, and  $\text{MnO}_2$ |TFA-BBA-CPB NCs|GCE treated with 1  $\mu\text{M}$  GSH in 0.1 M  $\text{K}_2\text{S}_2\text{O}_8$ .

**Table S1.** The respective energies of  $\text{CF}_3\text{CO}_2^-$ , BBA and  $\text{CsPbBr}_3$  and the adsorption energy.

Type	Energy Type	Energy magnitude (eV)	Absorption Energy $E_{ads}(eV)$
BBA	$E_{mol}$	-50.187068	
$\text{CF}_3\text{CO}_2^-$	$E_{mol}$	-41.705806	
$\text{CsPbBr}_3$	$E_{sub}$	-602.849280	
$\text{CsPbBr}_3+\text{BBA}$	$E_{total}$	-654.328450	-1.292102
$\text{CsPbBr}_3+\text{CF}_3\text{CO}_2^-+\text{BBA}$	$E_{total}$	-696.932700	-2.190546

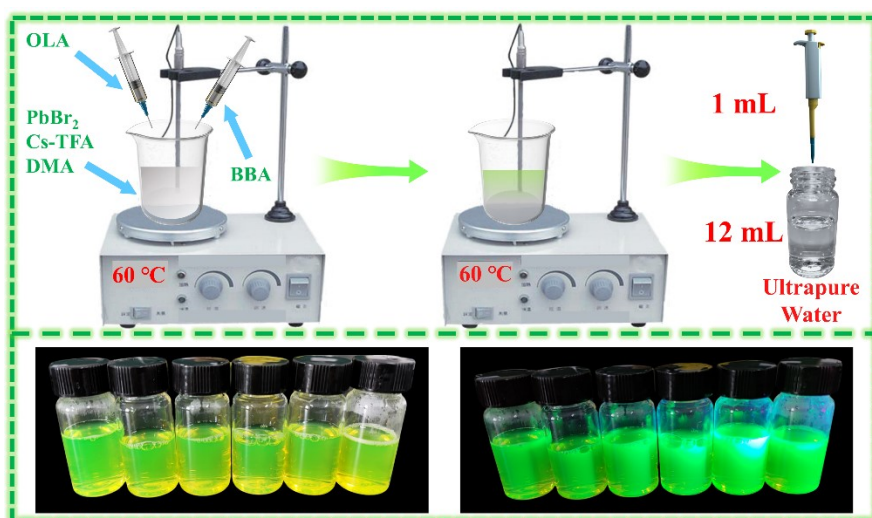


**Fig. S1** Synthesis method of TFA-BBA-CPB NCs in aqueous solutions.

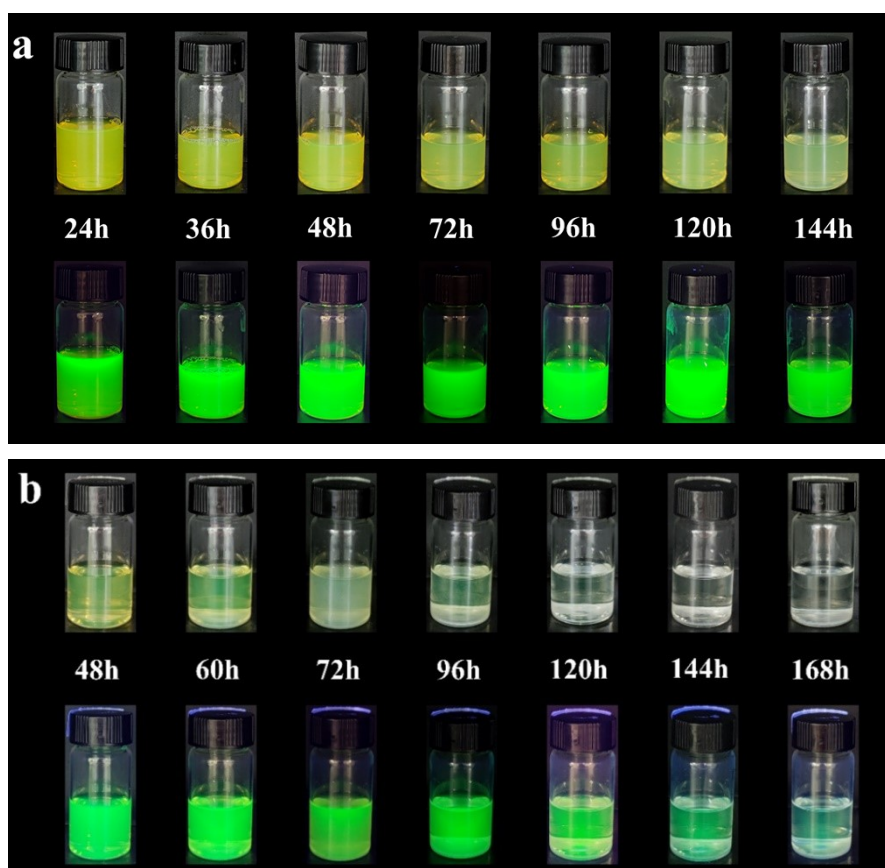


**Fig. S2** Sample photographs of (a) TFA-BBA-CPB NCs and (b) BBA-CPB NCs under natural light and UV light irradiation at 365 nm excitation wavelength with time.

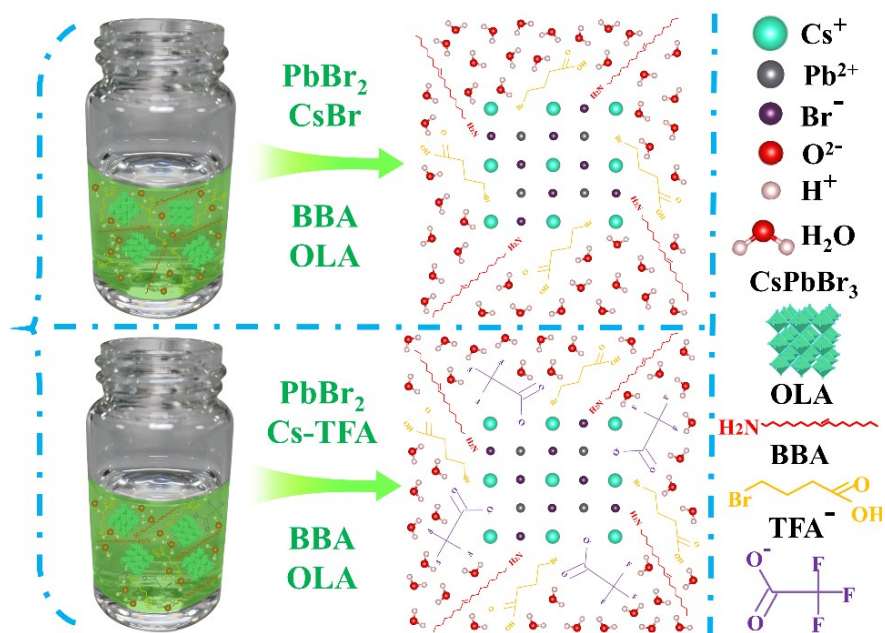


Fig. S3 Mechanistic investigations of TFA-BBA-CPB NCs and BBA-CPB NCs in aqueous solutions.

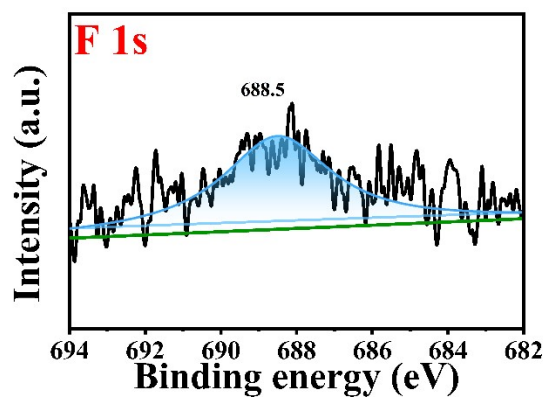
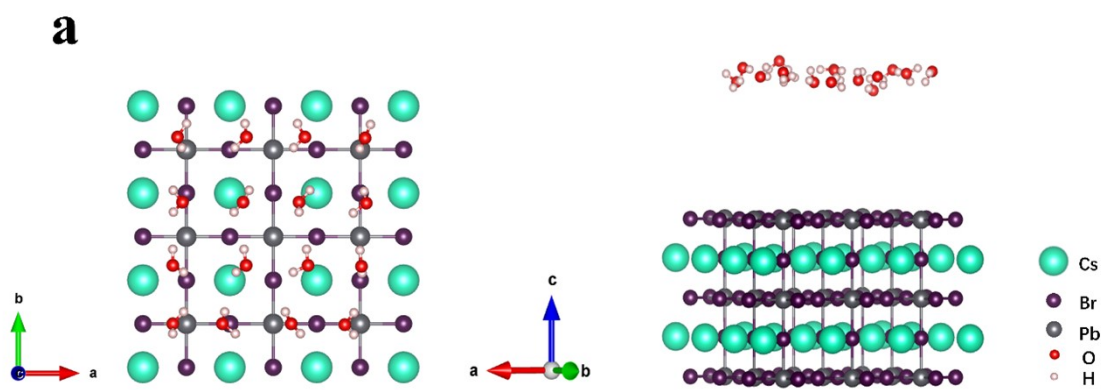
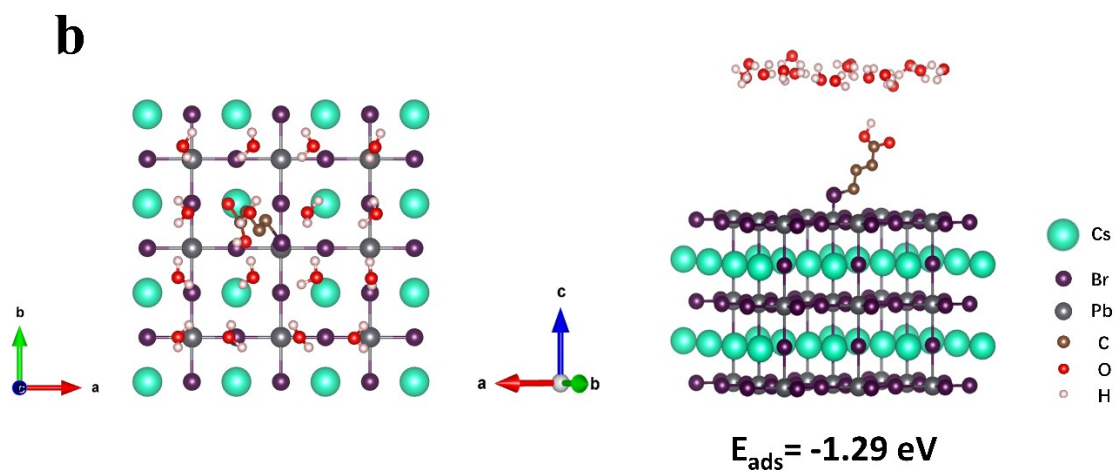
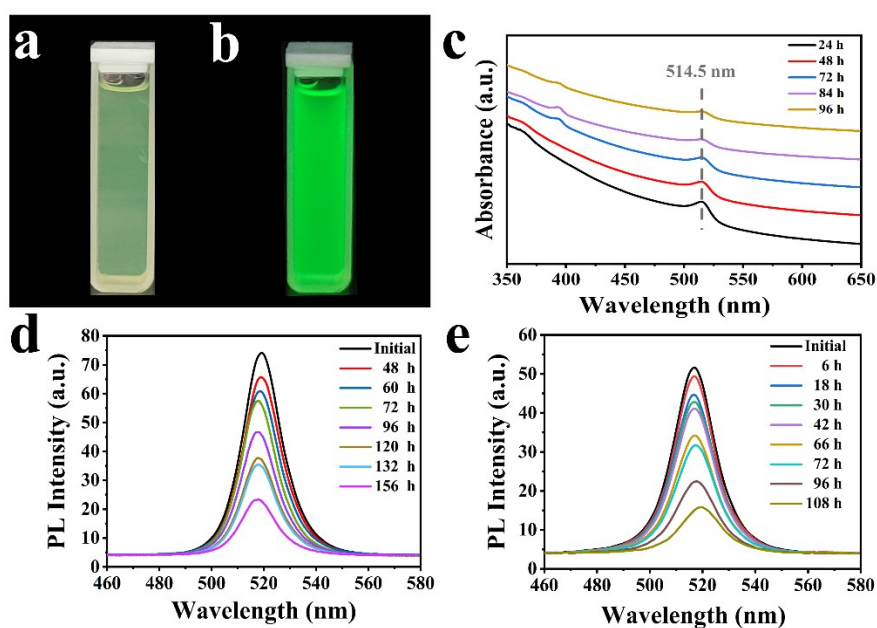


Fig. S4 XPS energy spectrum of F 1s in TFA-BBA-CPB NCs.





**Fig. S5** Crystal structure model of CPB NCs (a) before and (b) after the introduction of BBA.



**Fig. S6** Sample photographs of TFA-BBA-CPB NCs in quartz cuvette (a) under natural light and (b) UV irradiation at 365 nm excitation wavelength. (c) UV-vis absorption spectra and (d) the fluorescence emission spectra of TFA-BBA-CPB NCs. (e) The fluorescence emission spectra of BBA-CPB NCs in aqueous solutions.

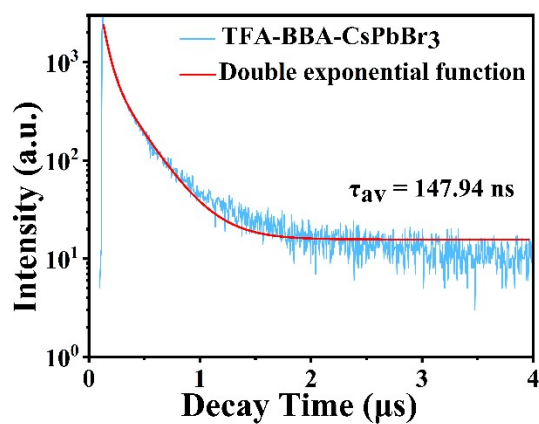


**Fig. S7** TRPL decay spectrum at 518 nm under the excitation of 375 nm for TFA-BBA-CPB NCs.

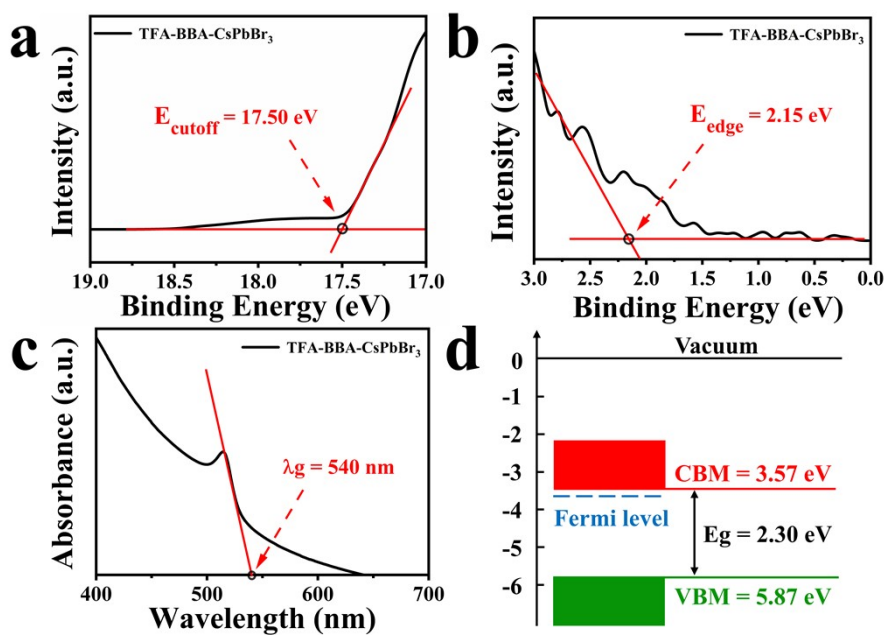


**Fig. S8** UPS spectra of TFA-BBA-CPB NCs in the photoemission (a) cutoff and (b) Fermi edge. (c) UV-vis absorption spectrum of TFA-BBA-CPB NCs. (d) Schematic representation of the band structure for TFA-BBA-CPB NCs at the interface.

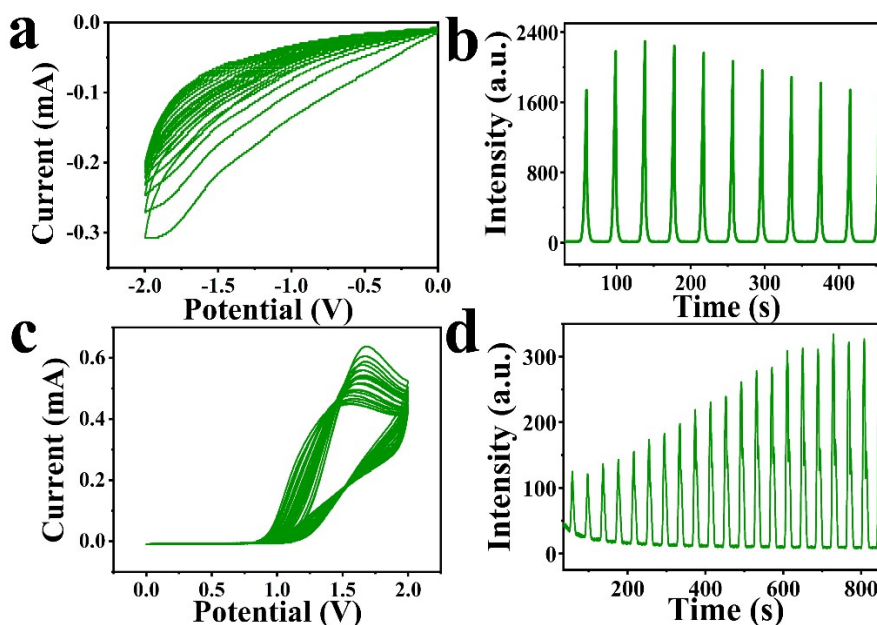


**Fig. S9** CVs of TFA-BBA-CPB NCs|GCE in air-free 0.1 M pH 7.4 PBS (a) containing 0.1 M  $K_2S_2O_8$  and (c) 0.2 M TEA at a scan rate of 0.1 V/s. ECL-time curve of TFA-BBA-CPB NCs with a potential window between 0.0 V and (b) -2.0 V or (d) +2.0 V.

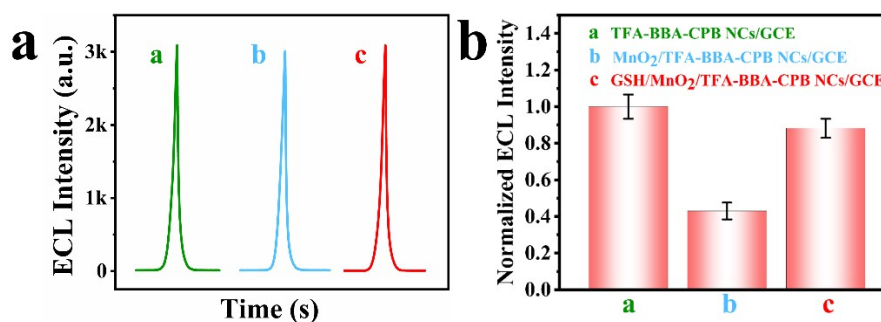


**Fig. S10** (a) ECL-time curves of TFA-BBA-CPB NCs (a) before, (b) during (the 14th circle), and (c) after ECL measurements. (b) The changes of ECL intensity of (a) TFA-BBA-CPB NCs|GCE, (b) MnO<sub>2</sub>|TFA-BBA-CPB NCs|GCE, and (c) MnO<sub>2</sub>|TFA-BBA-CPB NCs|GCE treated with 1  $\mu$ M GSH in 0.1 M  $K_2S_2O_8$ .

---

## Reference

- 1 S. Song, Y. Lv, B. Cao and W. Wang, *Adv. Funct. Mater.*, 2023, **33**, 2300493.
- 2 H. Zhu, Y. Pan, C. Peng, H. Lian and J. Lin, *Angew. Chem. Inter. Ed.*, 2022, **61**, e202116702.
- 3 N. Yan, Y. Gao, J. Yang, Z. Fang, J. Feng, X. Wu, T. Chen and S. (Frank) Liu, *Angew. Chem. Inter. Ed.*, 2023, **62**, e202216668.
- 4 J. Chen, D. Li, M. Su, Y. Xiao, H. Chen, M. Lin, X. Qiao, L. Dang, X. Huang, F. He and Q. Wu, *Angew. Chem. Inter. Ed.*, 2023, **62**, e202215930.
- 5 D. Yang, X. Li, W. Zhou, S. Zhang, C. Meng, Y. Wu, Y. Wang and H. Zeng, *Adv. Mater.*, 2019, **31**, 1900767.
- 6 H. Peng, W. Wu, Z. Huang, L. Xu, Y. Sheng, H. Deng, X. Xia and W. Chen, *Electrochem. Commun.*, 2020, **111**, 106667.
- 7 Z. Huang, S. Yu, M. Jian, Z. Weng, H. Deng, H. Peng and W. Chen, *Anal. Chem.*, 2022, **94**, 2341–2347.